SLAC-PUB-11700
February 2006
(A)

RF Gun Photo-Emission Model for Metal Cathodes Including Time Dependent Emission *

J. F. SCHMERGE, J. E. CLENDENIN, D. H. DOWELL, AND S. M. GIERMAN
SLAC, Stanford University, 2575 Sand Hill Rd
Menlo Park, CA 94025, USA

Abstract

The quantum efficiency from a metal cathode is strongly dependent on the field at the cathode due to the Schottky effect. Since the field is time dependent the quantum efficiency is also time dependent. Thus the laser pulse shape used to generate electrons in a photocathode rf gun is not the same as the electron bunch shape. In addition since the thermal emittance and quantum efficiency are related, the thermal emittance is also time dependent.

Contributed to the workshop on
The Physics and Applications of High Brightness Electron Beams 2005
October 9-14, 2005, Erice, Sicily, Italy

* Work supported by Department of Energy contract DE-AC02-76SF00515.

RF GUN PHOTO-EMISSION MODEL FOR METAL CATHODES INCLUDING TIME DEPENDENT EMISSION

J.F. SCHMERGE, J.E. CLENDENIN, D.H. DOWELL, AND S.M. GIERMAN

SLAC, Stanford University, 2575 Sand Hill Rd
Menlo Park, CA 94025, USA

The quantum efficiency from a metal cathode is strongly dependent on the field at the cathode due to the Schottky effect. Since the field is time dependent the quantum efficiency is also time dependent. Thus the laser pulse shape used to generate electrons in a photocathode rf gun is not the same as the electron bunch shape. In addition since the thermal emittance and quantum efficiency are related, the thermal emittance is also time dependent.

1. Motivation

1.1. *Introduction*

The emission from a photo-cathode rf gun depends on both the rf field and the incident laser pulse. In metal cathodes the rf field and image charges affects emission through the Schottky effect. All of these fields have fast time dependencies which must be accounted for to get an accurate model of the emitted electron pulse.

This paper describes the main time dependent effects and provides simple mathematical models to predict experimentally observed phenomena. The results apply to metal cathodes where the Schottky effect leads to an effective lowering of the work function. For those applications which require a flat top temporal electron beam, the time dependent cathode emission will lead to the use of drive laser pulses with asymmetric temporal shapes. In addition to the time dependent quantum efficiency (QE), it will be shown that the same time dependent fields result in a time dependent thermal emittance.

1.2. *Measurements*

Typically one of the first measurements performed while commissioning a photo-cathode gun is the measurement of charge vs laser phase. This type of measurement demonstrates the time dependent emission process due to the Schottky effect. All measurements reported here are conducted with a transverse flat-top laser profile.

A typical measurement performed at the SLAC Gun Test Facility (GTF) is shown in Figure 1 where the measured QE is plotted as a function of the laser phase for two different metal cathodes[1]. The QE is defined as the ratio of the number of electrons emitted to the number of incident photons. The charge is measured on a Faraday cup approximately 80 cm from the gun exit with a solenoid immediately downstream of the gun that has been adjusted to maximize the collected charge. Dark current is subtracted in the measurement to determine the photo emitted charge contribution. The laser energy is measured with a joule meter monitoring the energy downstream of a 1% pickoff.

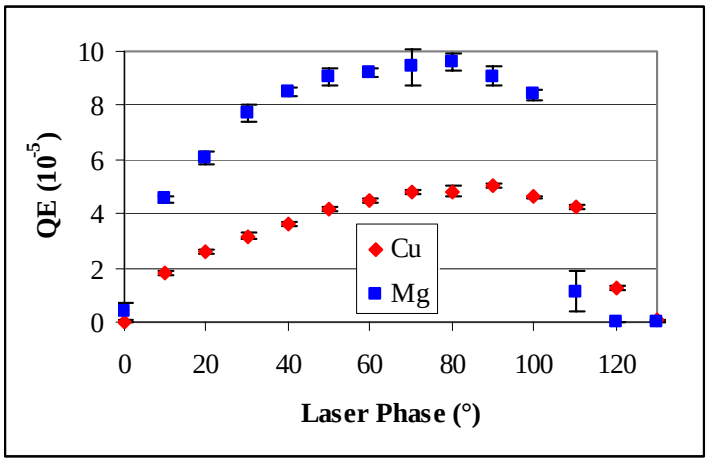

Figure 1. The measured QE as a function of laser phase for both Cu and Mg cathodes. A laser phase of 0° is defined as the zero crossing of the rf field at the cathode. The peak field at the cathode was 110 MV/m for the Cu cathode and 90 MV/m for the Mg cathode.

The Schottky scan in Figure 1 clearly demonstrates the importance of the rf field in the emission process. Equally important but not shown in Figure 1 is the effect of image charge. To demonstrate this effect the charge is measured as a function of laser energy. Figure 2 shows the result of such a measurement performed on the same Cu cathode but at a later time. Here the QE can be seen to be laser energy dependent. The linear fit is plotted and results in a QE of 6.6 10^{-5} which is roughly a factor of two higher than the QE shown in Figure 1. Other measurements on this and other Cu cathodes at the GTF have resulted in QEs ranging from 0.6-6 10^{-5} for an applied field of 120 MV/m and 30° laser phase. The reason for the variation of the QE has not been determined but it is suspected due to surface contaminants.

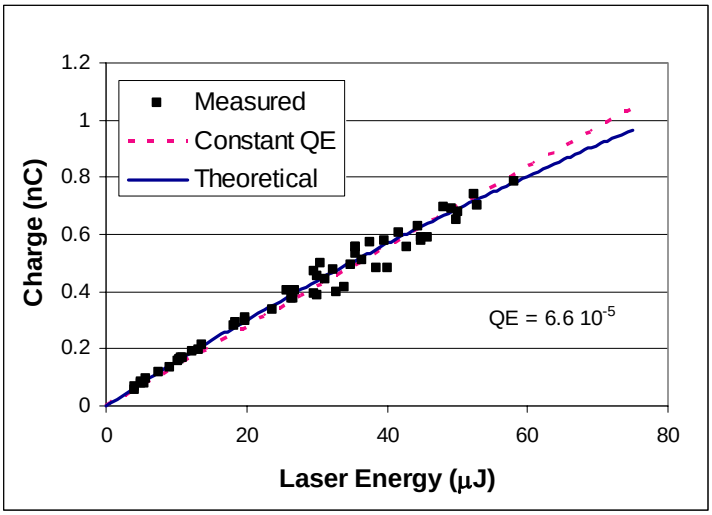

Figure 2. Measured charge as a function of laser energy for a Cu cathode at a laser phase of 40° and a peak field at the cathode of 110 MV/m. The dashed line is the linear fit to the measured data and the solid line is the fit using equation 1 which includes the effect of the image charge reducing the total field at the cathode. Due to the Schottky effect this leads to a reduction in QE for the tail of the pulse and thus the measured curve is not linear but rolls over as the laser energy is increased.

However, the linear fit always underestimates the charge for low laser energies and overestimates the charge for the highest laser energies. A better fit can be found by including the time dependent effects in a model that can accurately reproduce both experiments shown above.

2. Model

Typically, the QE from a metal cathode is assumed to behave as given in Equation 1[2] where the work function reduction due to the Schottky effect is defined in equation 2. $\Phi_{cathode}$ is the cathode work function with no applied field, hν is the laser photon energy and η_0 is a proportionality constant that can be determined from the slope of the charge vs laser energy plot at low charges.

The total field at the cathode is the superposition of the applied rf field and the field from the image charge where θ_{laser} is the laser phase and r is the laser beam radius at the cathode. Models for field emission include a field enhancement factor to account for geometrically enhanced surface fields at localized points. However, this model for photo-emission does not include a

field enhancement factor since the current is emitted over a large area and the average field should be equal to the applied field.

It is assumed in the derivation of equation 2 that the electron beam is a pancake beam and thus the space charge field is nearly independent of transverse position. If the space charge field depends on position then the QE will depend on both space and time[3,4]. However, in typical rf guns the head of the beam gains a small amount of energy over the duration of the laser pulse and moves only 10's of microns. Therefore, the large aspect ratio assumed for the pancake beam is nearly always satisfied.

For an applied field of 110 MV/m, the total field decreases to zero and suppresses further emission when the total charge exceeds 1.5 nC assuming a 2 mm diameter laser pulse. This is the space charge limit. The total charge is calculated by integrating the QE as shown in equation 3 where I_{laser} is the temporal power profile of the laser. The fit shown in figure 2 was produced by numerically integrating equations 1-3. Likewise equations 1-3 can be used to fit the data in figure 1. While the model fits the functional dependence on laser phase, the value of η_0 is different for the data in the two figures.

$$QE(t) = \eta_0 \left[h\nu - \left(\Phi_{cathode} - \Delta\Phi(t) \right) \right]^2 \tag{1}$$

$$\Delta\Phi(t) = \sqrt{\frac{e^3 \left(E_{RF} \sin\left(\omega_{RF} t + \theta_{laser} \right) - \dfrac{Q(t)}{\pi r_{cathode}^2 \varepsilon_0} \right)}{4\pi\varepsilon_0}} \tag{2}$$

$$Q(t) = \int_{-\infty}^{t} e \frac{I_{laser}(\tau)}{h\nu} QE(\tau)\, d\tau \tag{3}$$

However, equations 1-3 do not give a hint as to the theoretical maximum value of the QE or how the thermal emittance is related to the QE. A model that includes the electron energy distribution is needed to determine these parameters. In addition it was desired to consider why the QE varies with laser incidence angle and polarization. Thus a simplified model was developed to describe the emission process.

The basic model described below includes the following assumptions:

1. Electrons are emitted from the bulk material
2. Only electrons with sufficient momentum to overcome the work function surface barrier are emitted
3. Electrons in the cathode material exhibit a Fermi-Dirac electron energy distribution

4. The laser pulse bandwidth is ignored (except when investigating laser chirp effects)
5. Single photon absorption
6. The mean free path due to electron-electron scattering is assumed much longer than the optical skin depth.
7. Cathode has a flat planar surface
8. No surface effects except the laser beam reflection are included
9. No polarization effect other than reflectance

Electrons are assumed in thermal equilibrium until a photon is absorbed which raises the electrons kinetic energy. Since the mean free path is assumed infinite, the electrons that absorb a photon are assumed to escape the cathode if they reach the cathode surface and the longitudinal momentum is sufficient to overcome the barrier. The criterion for emission is given in equation 4 where p_z is the momentum perpendicular to the surface and E_b is the true barrier energy as defined in equation 6[5]. This requirement leads to an upper limit on the angle with respect to the surface normal, Φ_{max}, that an electron can approach the surface and still escape as given in equation 5 where E is the electron energy prior to absorption. This maximum angle is 10.9° for Cu and 19.7° for Mg assuming a field at the cathode of 120 MV/m and a 263 nm photon. Figure 3 is an energy level diagram for both Cu and Mg showing the barrier energy and the minimum required energy for an electron to absorb a photon and emit as defined in equation 7.

$$p_z \geq \sqrt{2mE_b} \tag{4}$$

$$\cos\Phi_{\max} = \sqrt{\frac{E_b}{E+h\nu}} \tag{5}$$

$$E_b \equiv E_F + \Phi_{cathode} - \Delta\Phi \tag{6}$$

$$E_{\min} \equiv E_b - h\nu \tag{7}$$

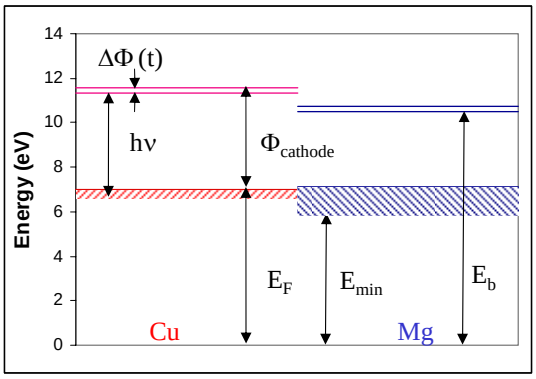

Figure 3. An Energy level diagram for Cu is shown on the left and Mg on the right. The lowest solid line is the Fermi Energy and for T=0 K is the uppermost electron energy state in the metal. The upper solid line is the work function plus the Fermi level and the line immediately below it represents the Schottky effect reduction. This is the real electron barrier the electron must overcome to be emitted. The cross hatched area represents the electrons with sufficient energy to escape.

Since e-e scattering is effectively ignored, the depth below the cathode surface at which the electrons absorb a photon is irrelevant in this model. Of course the number of photons penetrating into the metal exponentially decays with the skin depth and the deeper the electron are generated the less likely they will reach the surface with sufficient energy to escape due to electron-electron scattering. However, from the simple model assuming emission is independent of depth, a reasonable account of photo-emission can be established.

2.1. *Quantum Efficiency*

The QE is then the number of electrons that could escape divided by the total number of electrons summed over energy and the solid angle times the fraction of laser energy actually absorbed in the cathode. With this in mind and the physical model described above the quantum efficiency can be described as the integral shown in equation 8 where $N_{electron}$ is the electron energy distribution which is assumed a Fermi-Dirac distribution and R is the power reflectance of the laser which is angle and polarization dependent..

$$QE = (1-R)\frac{\int_{E_{\min}}^{E_b}\int_0^{\Phi_{\max}}\int_0^{2\pi} N_{electron}\sin\Phi d\theta d\Phi dE}{\int_0^{E_b}\int_0^{\pi}\int_0^{2\pi} N_{electron}\sin\Phi d\theta d\Phi dE} \tag{8}$$

An analytic solution for equation 8 can be found if we assume the temperature is 0 K. The result is given in equation 9 with E_k defined in equation 10. Equation 8 must be numerically integrated or solved approximately for non-zero temperatures. Higher temperatures lead to higher QEs since more electrons have sufficient energy to participate in the emission process. However, it typically requires very high temperatures to produce order of magnitude increases in the QE except when the photon energy is on the same order as the work function as seen in Figure 4. The theoretical QE is plotted as a function of laser wavelength in Figure 4 for Cu along with the measured QE with near zero applied field[6]. The theoretical QE is nearly a factor of three greater than the measured value. This is the same factor that the theoretical QE is reduced if the finite mean free path is included in the model[7].

$$QE = (1-R)\frac{\left(1-2\left(E_b/E_k\right)^{1/2}+\left(E_b/E_k\right)\right)}{2\left(E_F/E_k\right)} \tag{9}$$

$$E_k \equiv E_F + h\nu \tag{10}$$

This expression gives 16 10^5 and 21 10^5 for the QE of Cu and Mg respectively at room temperature under identical conditions as the experimental results in Figure 1 at 30° laser phase. Although the work function of Mg is nearly 1 eV lower than Cu, the QE is not significantly higher due to the much higher reflectivity at 263 nm. The Cu reflectivity is only 34%[8] while Mg is approximately 92%[9]. Our model QE values are a factor of 6 and 3 higher for the Cu and Mg measurements in figure 1 and 3 times higher than the QE shown in figure 2. Most of this discrepancy can be attributed to assuming an infinite mean free path as discussed above. The rest is assumed due to localized contaminants on the surface[6] which creates a spatially varying work function and surface reflectivity. Methods of cleaning the cathode in situ to raise the measured QE to the theoretical value are under investigation.

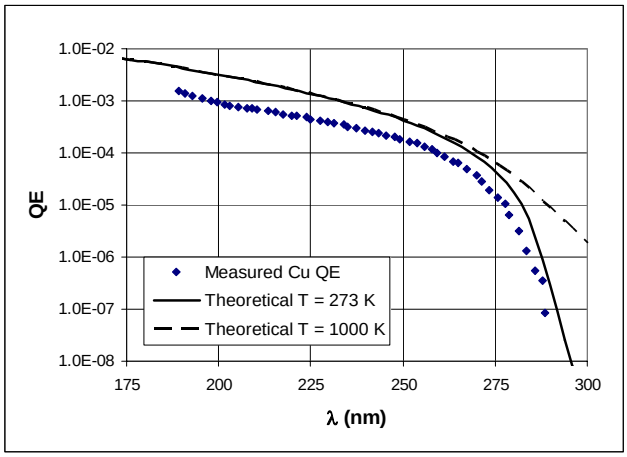

Figure 4. The QE as a function of laser wavelength is plotted for a Cu cathode at two different temperatures. Diamonds points are measured data for a Cu cathode after cleaning with 1 keV H^+ ions.

Interestingly equation 9 can be reduced to equation 1 where an approximate solution for η_0 can be derived. The expression for η_0 is a function of E_F, $h\nu$, $\Phi_{cathode}$ and $\Delta\Phi$ but is not reported here since it is cumbersome and not particularly useful. However, the model has the same functional dependence as equation 1 and the experiments, but the predicted value of the QE is larger than is measured at the GTF.

The QE is time dependent due to the Schottky effect. As the field at the cathode increases, the barrier energy decreases and the QE will increase because more electrons in the metal have sufficient energy to emit. Likewise the QE will decrease if the field at the cathode is decreased. For typical parameters at the GTF it requires approximately a 15% change in the cathode field to change the QE by 10%.

The physical model also provides some insight into the response time of the cathode. Electrons that absorb a photon near the surface can be emitted immediately while electrons that absorb photons below the surface must travel to the surface before escaping. The response time constant is estimated in equation 11 where δ is the optical skin depth. For Cu at 263 nm the time constant is approximately 6.0 fs and for Mg the time constant is only 4.8 fs due to the shorter skin depth.

$$\tau \approx \frac{\delta}{\sqrt{\frac{2E_k}{m}}} \tag{11}$$

Looking at figure 4 it appears that one can achieve much higher QEs by using a photon energy that significantly exceeds the cathode work function. While this is true it only tells part of the story since the thermal emittance and QE are related. The reason the QE rises as the wavelength is decreased is that an increased number of electrons have sufficient energy to escape from the metal. This also leads to larger amounts of excess energy once they are emitted or in other words a larger thermal emittance.

2.2. *Thermal Emittance*

The thermal emittance is a measure of the transverse energy of the electrons at the cathode surface. The definition of normalized thermal emittance is given in equation 12. Assuming the electron momentum is independent of position (correlated term is zero) on the cathode, the thermal emittance can be expressed as shown in equation 13 where the sum is performed only over the emitted electrons. The electron density distribution on the cathode, f(ρ,θ), is identical to the laser photon density distribution for a cathode with uniform QE.

$$\varepsilon_{nthermal} \equiv \frac{1}{mc}\sqrt{\left\langle x^2\right\rangle\left\langle p_x^2\right\rangle - \left\langle xp_x\right\rangle^2} \tag{12}$$

$$\varepsilon_{nthermal} \equiv \frac{1}{mc}\sqrt{\frac{\int_0^{r_{cathode}}\int_0^{2\pi} f(\rho,\theta)\rho^3\cos^2\theta d\theta dr \int_{E_{\min}}^{E_b}\int_0^{\Phi_{\max}}\int_0^{2\pi} N_{electron}\, p_x^2 \sin\Phi d\theta d\Phi dE}{\int_0^{r_{cathode}}\int_0^{2\pi} f(\rho,\theta)\rho d\theta dr \int_{E_{\min}}^{E_b}\int_0^{\Phi_{\max}}\int_0^{2\pi} N_{electron}\sin\Phi d\theta d\Phi dE}} \tag{13}$$

For a flat-top laser profile and a temperature of 0 K the thermal emittance can be expressed as shown in equation 14. Non-zero temperatures require approximate or numerical solutions. The thermal emittance as a function of laser wavelength is plotted in Figure 5 for a 1 mm flat-top pulse. Temperature effects are significant when the photon energy is greater than the work function. The thermal emittance increases as the temperature is increased due to the additional energy the electrons possess after emission. Likewise decreasing the work function will increase the thermal emittance. Thus the thermal emittance for Cu and Mg are calculated to be 0.25 μm/mm and 0.46 μm/mm respectively using a 263 nm photon.

$$\varepsilon_{nthermal} = \frac{r_{cathode}}{2}\sqrt{\frac{E_k}{mc^2}}\sqrt{\frac{\left(1-2\left(E_b/E_k\right)^{1/2}+2\left(E_b/E_k\right)^{3/2}-\left(E_b/E_k\right)^2\right)}{3\left(1-2\left(E_b/E_k\right)^{1/2}+\left(E_b/E_k\right)\right)}} \tag{14}$$

The theoretical thermal emittance is roughly a factor of two less than is typically measured[1,10,11]. Scattering will decrease the theoretical emittance due to a decrease in the average energy of the emitted electrons. The discrepancy could be due to acceleration from the rf field inside the metal before emission, surface roughness, non-uniform emission or other effects. Surface roughness can increase the thermal emittance since the average transverse momentum of an emitted electron is increased because the emitted electrons are peaked normal to the tilted surface. In addition, the rf field which is also normal to the tilted surface will add transverse energy.

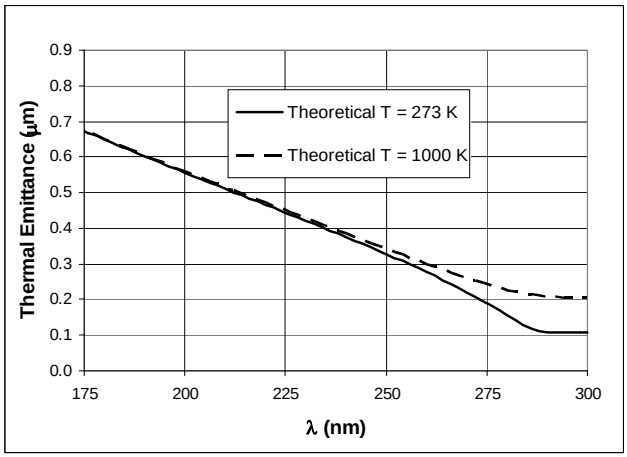

Figure 5. The thermal emittance as a function of laser wavelength is plotted for a Cu cathode at two different temperatures.

It should be clear from equations 9 and 14 that the thermal emittance and QE are related. One can combine figures 4 and 5 to give the thermal emittance as a function of QE. Figure 6 shows the cost in thermal emittance for increases in QE. Increasing the QE from 10^{-4} to 10^{-3} nearly doubles the thermal emittance. Based on these calculations the LCLS will shift the Ti:sapphire laser wavelength from 790 nm to 765 nm and use the third harmonic at 255 nm. This increases the expected QE by more than a factor of two while only increasing the predicted thermal emittance by 20%.

The thermal emittance is also clearly time dependent. If the field at the cathode increases the barrier energy decreases and the thermal emittance increases. Likewise if the field decreases the thermal emittance decreases. The percent change in thermal emittance is not as dramatic as the QE variation but depending on the pulse length and charge it can be significant. For typical parameters at the GTF a 70% change in field is required to produce a 10% change in the thermal emittance.

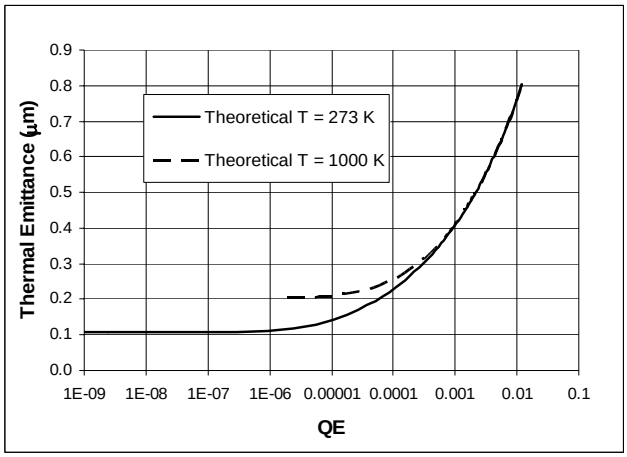

Figure 6. The thermal emittance as a function of QE is plotted for a Cu cathode at two different temperatures.

3. Laser and Electron Pulse Shape

Since the barrier energy is time dependent due to the Schottky effect, the QE and the thermal emittance are both time dependent. Of course the QE variation is more dramatic as is evident from figures 4 and 5.

When operating well below the space charge limit the head of the beam sees a lower field at the cathode than the tail due to the rising rf field. Thus the barrier energy is higher at the head and the QE and thermal emittance are smaller. When operating near the space charge limit just the reverse occurs since the field at the cathode for the tail is nearly zero. It is possible to operate in the middle where the decrease in the space charge field nearly cancels the rise in the rf field. At this point the Schottky effect is nearly constant and so are the QE and the thermal emittance. However, this is only valid at a specific charge and for a specific pulse shape which depends on the rf field, laser phase and beam radius.

Typically, the Schottky effect is not included in rf gun simulations and the electron beam pulse reproduces the drive laser pulse. In the LCLS where a very low emittance beam is required, the electron pulse shape helps determine the final transverse emittance due to space charge forces. It is assumed in the simulations that the electron beam will have the same temporal shape as the laser pulse that generates the beam. However, as shown earlier the Schottky effect has a large effect on emission from metal cathodes. Thus both the transverse and longitudinal phase space distributions will be affected.

Equations 1-3 are numerically integrated to determine the electron beam shape for a given laser pulse shape. Figure 7 shows the resulting electron beam pulse shape with a flat-top laser pulse and also the required laser pulse shape to generate a flat-top electron beam shape for the nominal LCLS case. With a flat top laser pulse the electron beam has about a -1 A/ps slope which is highly dependent on the beam parameters. For example a decrease in beam radius from 1.2 to 1 mm would change the slope to approximately -2 A/ps. The electron beam slope can be corrected by using a laser with an asymmetric pulse shape to compensate for the decrease in QE. A laser with an approximately 10% increase over the pulse will produce a flat electron beam. Of course the slope would need to increase to about 20% if the laser diameter were decreased to 1 mm.

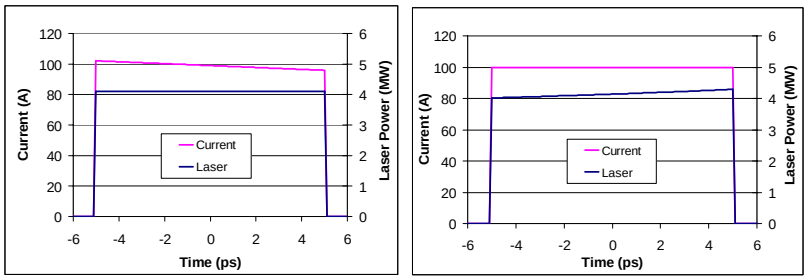

Figure 7. The electron beam pulse for a flat-top laser pulse is shown on the left and the required laser pulse shape to produce a flat-top electron beam is shown on the right. The nominal LCLS parameters include a laser wavelength of 255 nm, 120 MV/m rf amplitude, 30° laser phase, total charge of 1 nC and laser beam radius of 1.2 mm.

As mentioned earlier it is possible to produce a flat electron beam with a flat laser pulse but this only occurs for a specific set of parameters. Changing any single parameter leads to a time dependent QE. Another parameter which can be manipulated is the laser beam chirp. Changing the laser wavelength along the pulse can flatten the QE. Although one can not simultaneously compensate both the QE and thermal emittance with laser chirp exactly, it is possible to reduce the variation for both QE and thermal emittance to the order of 2% or less. A laser chirp of -0.1 nm/ps is sufficient to generate a flat electron pulse with a flat laser pulse for the nominal LCLS case.

4. Conclusions

Time dependent fields at the cathode lead to time dependent QE and thermal emittance through the Schottky effect. A simple model that includes the time dependent fields can be used to predict the QE and thermal emittance. The model overestimates the quantum efficiency most likely because the model does

not properly include e-e scattering in the metal and also does not account for surface contaminants which may decrease the QE at localized positions. The model underestimates the thermal emittance possibly because it does not include acceleration prior to emission and surface roughness.

Due to the time dependent QE, the electron pulse shape is not identical to the laser pulse shape. Thus the laser pulse shape must be shaped to produce the desired electron pulse shape. If the charge is much less than the space charge limit the laser power will need to decrease during the pulse to compensate for the increase in QE. If the charge is close to the space charge limit the laser power will need to increase as time increases. When the space charge field temporal variation cancels the applied rf field temporal variation the QE is independent of time.

The charge, rf field amplitude, laser phase, or beam diameter will all affect the final electron pulse shape. In addition the laser beam wavelength affects the QE so the chirp of the laser is also important. However, the Schottky effect is typically not included in electron beam simulations so the electron beam shape at the cathode is incorrect. Thus the longitudinal space charge term will not be properly calculated by the codes and the beam will evolve differently from the simulation. Thus for those experiments that rely on simulations to design a beam-line that delivers a desired phase space distribution, the Schottky effect with a metal cathode should be included.

Acknowledgments

This work supported by the U.S. Department of Energy under contract number DE-AC02-76SF00515.

References

1. J.F. Schmerge et al, Proceedings of the 2004 FEL Conference, pp. 205-208, 2004 and SLAC-PUB-10763, 2004.
2. T. Srinivasan-Rao, J. Fischer and T. Tsang, Journal of Applied Physics, Vol. 69, no. 5, pp 3291-3296, 1991.
3. J. Rosenzweig et al, Nuclear Instruments and Methods Vol. A341, pp. 379-385, 1994.
4. J.L. Adamski et al, SPIE Vol. 2988, pp 158-169, 1997.
5. M. Cardona and L. Ley, Photoemission in Solids I, Springer-Verlag, pp 22-23, 1978.
6. D.H. Dowell et al, to be published in the 2005 FEL Conference Proceedings, Stanford, CA, August, 2005.
7. J.Smedley, to be published in These Proceedings.
8. M.J. Weber, “Handbook of Optical Materials”, pg 317, 2002.

9. E.D. Palik, “Handbook of Optical Constants of Solids III”, pg 239, 1998.
10. W.S. Graves et al, Proceedings of the 2001 Particle Accelerator Conference, pp. 2227-2229, 2001.
11. J. Yang et al, Proceedings of the 2002 European Particle Accelerator Conference, pp. 1828-1830, 2002.